Accepted Manuscript

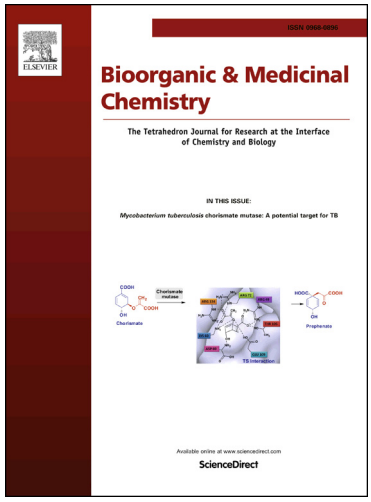

Structural modifications of diarylpyrimidines (DAPYs) as HIV-1 NNRTIs: synthesis, anti-HIV activities and SAR

Huan-Huan Lu, Ping Xue, Yuan-Yuan Zhu, Xiu-Lian Ju, Xiao-Jiao Zheng, Xun Zhang, Ting Xiao, Christophe Pannecouque, Ting-Ting Li, Shuang-Xi Gu

PII: S0968-0896(17)30218-3
DOI: http://dx.doi.org/10.1016/j.bmc.2017.03.009
Reference: BMC 13605

To appear in: *Bioorganic & Medicinal Chemistry*

Received Date: 1 February 2017
Revised Date: 4 March 2017
Accepted Date: 5 March 2017

Please cite this article as: Lu, H-H., Xue, P., Zhu, Y-Y., Ju, X-L., Zheng, X-J., Zhang, X., Xiao, T., Pannecouque, C., Li, T-T., Gu, S-X., Structural modifications of diarylpyrimidines (DAPYs) as HIV-1 NNRTIs: synthesis, anti-HIV activities and SAR, *Bioorganic & Medicinal Chemistry* (2017), doi: http://dx.doi.org/10.1016/j.bmc.2017.03.009

This is a PDF file of an unedited manuscript that has been accepted for publication. As a service to our customers we are providing this early version of the manuscript. The manuscript will undergo copyediting, typesetting, and review of the resulting proof before it is published in its final form. Please note that during the production process errors may be discovered which could affect the content, and all legal disclaimers that apply to the journal pertain.

ACCEPTED MANUSCRIPT

Structural modifications of diarylpyrimidines (DAPYs) as HIV-1 NNRTIs: synthesis, anti-HIV activities and SAR

Huan-Huan Lu[a], Ping Xue[a], Yuan-Yuan-Zhu[b,*], Xiu-Lian Ju[a], Xiao-Jiao Zheng[a]; Xun Zhang[a], Ting Xiao[a], Christophe Pannecouque[c,*], Ting-Ting Li,[d] Shuang-Xi Gu[a,*]

[a] *Key Laboratory for Green Chemical Process of Ministry of Education, School of Chemical Engineering & Pharmacy, Wuhan Institute of Technology, Wuhan 430205, China*

[b] *School of Chemistry and Environmental Engineering, Wuhan Institute of Technology, Wuhan 430205, China*

[c] *KU Leuven, Department of Microbiology and Immunology, Laboratory of Virology and Chemotherapy, Rega Institute for Medical Research, B-3000 Leuven, Belgium*

[d] *Institute of Hydrobiology, Chinese Academy of Sciences, Wuhan 430072, China*

[*]Corresponding Authors:

E-mail: yyzhu531@163.com; christophe.pannecouque@kuleuven.be; shuangxigu@163.com.

Abstract

30 new analogues of diarylpyrimidines were synthesized for further structural modifications, involving not only the linker but also the wing α of DAPYs. The anti-HIV-1 activities of all target molecules were evaluated, and most of them exhibited potent anti-HIV-1 (WT) activities and low cytotoxicities. Among which, compound **4g** showed excellent activities against WT HIV-1 with an EC_{50} value of 5.8 nM and SI of up to 26,034. Another compound **4ab** bearing a novel pyridinyl Wing α also displayed attractive activities. The structure-activity relationship (SAR) study was also summarized.

Keywords: AIDS; anti-HIV; diarylpyrimidines; nonnucleoside reverse transcriptase inhibitors; SAR

ACCEPTED MANUSCRIPT

ACCEPTED MANUSCRIPT

1. Introduction

Acquired immunodeficiency syndrome (AIDS) is a global infectious disease caused by human immunodeficiency virus (HIV) infection. According to the data from UNAIDS reported on July 11th, 2016, the situation is still unoptimistic: in 2015, 36.7 million people lived with HIV, 2.1 million people were newly infected with HIV, and there were as many as 1.1 million of AIDS-related deaths.[1] So far there is no cure or effective vaccine against HIV/AIDS. Highly active antiretroviral therapy (HAART) still occupies a dominant position in combating AIDS in spite of its existing limitations such as complicated dosing, intolerable toxicities, caustic adherence.[2-4] Nonnucleoside reverse transcriptase inhibitors (NNRTIs), known as one of the indispensable components of HAART for specifically inhibiting HIV-1 reverse transcriptase (RT), have received wide attention due to their potent antiviral activity, high specificity and low cytotoxicity.[5, 6]

Among various structurally diverse classes of NNRTIs,[7, 8] diarylpyrimidines (DAPYs) have been recognized as one of the most successful families of NNRTIs developed so far owing to their excellent potency against both HIV-1 wild-type (WT) and mutant strains.[9] In DAPYs series, the most important representatives etravirine (TMC125, **1**, Fig. 1) and rilpivirine (TMC278, **2**, Fig. 1) have been approved by the U.S. Food and Drug Administration (FDA) in 2008 and 2011, respectively.[10, 11] Since the right wing of the DAPY structure was identified as the essential pharmacophore, the further modifications were mainly focused on the structural diversity of the linker between the left phenyl ring and the central pyrimidine ring. Until present, nearly all of the DAPY derivatives share a common characteristic: the monoatomic linker (C, O, S, or N) between Wing II and the central pyrimidine ring.[12-16]

In 2015, based on the concept of improving conformational flexibility and positional adaptability, we designed a new family of DAPYs featuring a diatomic linker, named *CH$_2$NH*-DAPYs (**3**, Fig. 1),[17] Most of the designed molecules showed excellent activities against wild-type (WT) HIV-1. Herein, in a continuing effort to develop new HIV-1 NNRTIs, we have made structural modifications of *CH$_2$NH*-DAPYs to design 30 compounds, involving not only the modifications of the linker but also of the wing α of DAPYs.

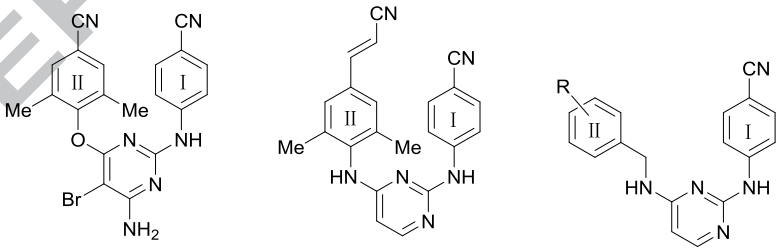

Fig. 1 Structures of DAPYs

2. Results and discussion

2.1 Synthesis

The target compounds **4a-ac** were prepared according to our published methods.[17-19] The synthetic route of target molecules is given in Scheme 1. In this route, the key intermediate 4-((4-chloropyrimidin-2-yl)amino)benzonitrile (**8**) was prepared in three successive steps from thiouracil (**5**) including methylation, solvent-free nucleophilic substitution, and chlorination. Subsequently, intermediate **8** reacted with the corresponding alcohols, amine and thiol to afford the

ACCEPTED MANUSCRIPT

product **4a-x**, **4aa-4ab** and **4ac** via reaction *d*, *e*, and *f*. Furthermore, we also tried to carry out the amination reaction of **8** with aqueous ammonia in dimethylformamide (DMF) at 140 °C. However, the unexpected by-product **4ad** was generated, which was ascribed to the existence of dimethylamine produced by the decomposition reaction of DMF under 140℃.[20]

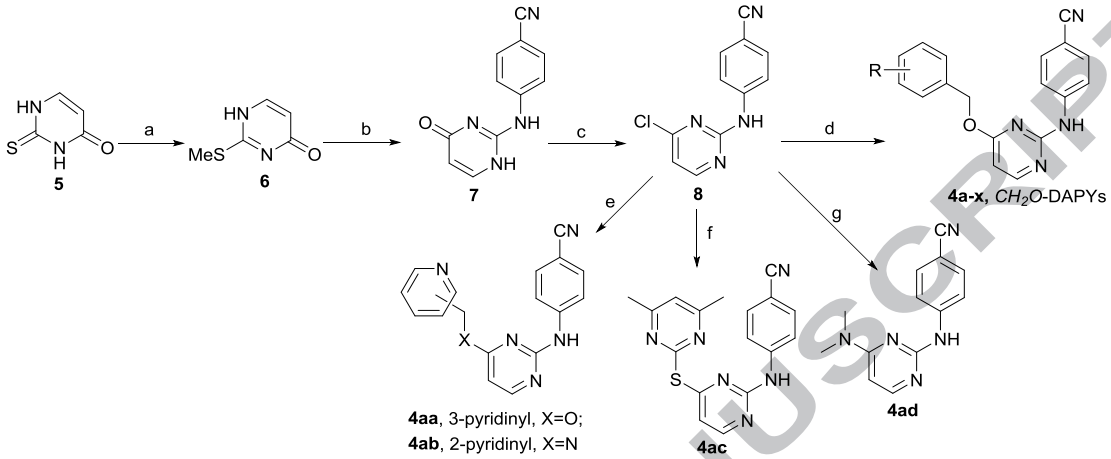

Compd	R-Ph	Compd	R-Ph	Compd	R-Ph	Compd	R-Ph
4a	2-Cl-Ph	**4h**	3-F-Ph	**4o**	4-OCH_3-Ph	**4v**	3-CN-Ph
4b	3-Cl-Ph	**4i**	4-F-Ph	**4p**	2-CF_3-Ph	**4w**	4-CN-Ph
4c	4-Cl-Ph	**4j**	2-CH_3-Ph	**4q**	3-CF_3-Ph	**4x**	Ph
4d	2-Br-Ph	**4k**	3-CH_3-Ph	**4r**	3,5-diMeO-Ph	**4y**	1-Naph
4e	3-Br-Ph	**4l**	4-CH_3-Ph	**4s**	5-F-2-Br-Ph	**4z**	2-Naph
4f	4-Br-Ph	**4m**	2-OCH_3-Ph	**4t**	2-F-4-Br-Ph		
4g	2-F-Ph	**4n**	3-OCH_3-Ph	**4u**	2-CN-Ph		

Scheme 1. Synthesis of target molecules **4a-ad**. Reagents and conditions: a) MeI, NaOH, H_2O, rt, 14 h; b) 4-cyanoaniline, 180–190℃, 10 h; c) $POCl_3$, reflux, 0.5 h; d) R-PhCH_2OH or naphthalenemethanol, NaOH, DMSO, 80℃; e) pyridin-3-yl-methanol, or pyridin-2-yl-methanamine, NaOH, DMSO, 80℃; f) 4,6-dimethylpyrimidine-2-thiol, NaOH, DMSO, 80℃; g) aqueous ammonia, DMF, 140℃ (**4ad** was a by-product).

2.2 Biological activity

The anti-HIV activity and cytotoxicity of compounds **4a-ad** were assessed using the MT-4/MTT method.[21, 22] Five FDA-approved drugs, including nevirapine, delavirdine, efavirenz, azidothymidine, and etravirine, were also evaluated as reference drugs. The compounds were assayed for their anti-HIV activity against wild-type (WT) HIV-1 (strain III_B), RT mutant E138K, double RT mutant (K103N + Y181C), as well as HIV-2 (strain ROD). The results, expressed as CC_{50} (50% cytotoxic concentration), EC_{50} (50% HIV-1 replication inhibitory concentration) and SI (selectivity index given by the CC_{50}/EC_{50} (III_B) ratio) values were listed in Table 1.

As shown in Table 1, most of target molecules displayed good to excellent activities against wild-type (WT) HIV-1. The four most potent compounds (**4g**, **4k**, **4r**, and **4ab**) displayed rather potent WT HIV-1 inhibitory activities with EC_{50} values lower than 9 nM, which were comparable to the FDA-approved efavirenz, etravirine and azidothymidine, and lower than the other two reference drugs nevirapine, and delavirdine. Moreover, 14 target molecules showed excellent selectivity index of higher than 1000.

ACCEPTED MANUSCRIPT

Table 1. Anti-HIV activities and cytotoxicity in MT-4 cells of **4a-ad**[a]

Compd	EC_{50} (μM)[b]			ROD (μM)[c]	CC_{50} (μM)[d]	SI[e]
	III_B	E138K	K103N+Y181C			
4a	0.034	>146	>146	>146	146	4424
4b	0.049	>153	>153	>153	153	3122
4c	0.840	>156	>156	>156	156	186
4d	0.036	>130	>130	>130	130.00	3611
4e	0.048	5.0	>221	>221	221	4604
4f	4.7	>16	>16	>16	16	3.4
4g	0.0058	0.30	>151	>151	151	26034
4h	0.014	1.88	>105	>105	105	7500
4i	0.92	>81	>81	>81	81	88
4j	0.16	>12	>12	>12	12	75
4k	0.0088	1.18	>30	>30	30	3409
4l	0.16	7.2	>81	>81	81	495
4m	0.027	2.1	>8.9	>8.9	8.9	356
4n	0.025	1.1	>118	>118	118	4720
4o	1.0	>102	>102	>102	102	102
4p	1.7	>173	>173	>173	173	102
4q	0.61	>118	>118	>118	118	193
4r	0.0089	0.23	>44	>44	44.21	4944
4s	0.039	>190	>190	>190	190	4872
4t	0.22	35.81	>141	>141	141	641
4u	0.014	>113	>113	>113	113	8071
4v	0.18	>4.1	>4.1	>4.1	4.1	23
4w	1.4	>209	>209	>209	209	149
4x	0.022	1.8	>13	>13	13	591
4y	0.015	0.30	>7.7	>7.7	7.7	513
4z	0.17	10	>212	>212	212	1247
4aa	0.77	>6.4	>6.4	>6.4	6.4	8
4ab	0.0076	0.24	>8.5	>8.5	8.5	1118
4ac	27	>224	>224	>224	224	8
4ad	>34	>34	>34	>34	34	<1
Nevirapine	0.21	0.24	>15	—	>15	72
Efavirenz	0.0073	0.0052	0.16	—	6.3	868
Etravirine	0.0042	0.017	0.046	—	1.9	455
Azidothymidine	0.011	0.0066	0.0089	—	7.5	662
Delavirdine	0.037	0.076	>23	—	23	628

[a] Data represent the mean of at least three independent experiments.

[b] Compound concentration required to protect MT-4 cells against HIV-1-induced cytopathogenicity by 50%.

[c] Compound concentration required to protect MT-4 cells against HIV-2-induced cytopathogenicity by 50%.

[d] Compound concentration that decreases the uninfected MT-4 cell viability by 50%.

[e] Selectivity index: CC_{50}/EC_{50} (III_B) ratio .

ACCEPTED MANUSCRIPT

The 30 target molecules are chemically and biologically diverse. Herein, their structure-activity of relationship (SAR) against WT HIV-1 was summarized. Compound **4a-i** were characterized by the presence of a mono-halogen substituent such as Cl, Br, or F. Compared with the non-substituted compound **4x**, introduction of Cl or Br seemed to be unfavorable to the WT HIV-1 inhibitory activities, being demonstrated by **4a-f** with more or less reduced activities. Notably, the *para*-Cl, -Br and -F were all hugely detrimental to the potency, and the activities of corresponding compounds **4c**, **4f**, and **4i** were decreased to micromolar level. Encouragingly, *ortho*-F (**4g**, EC_{50} = 5.8 nM, SI = 26034) and meta-F (**4h**, EC_{50} = 14 nM, SI = 7500) enhanced the activities significantly, combined with their low cytotoxicity, resulted in extremely high SI. It is not unexpected as it is well known that fluorine atom usually plays a very important role in medicinal chemistry due to its versatility.[23, 24] For all mono-halogen-substituted compounds, the position priority abided by the rules as follows: ortho- > meta- > -para, for example, **4a** > **4b** > **4c**; **4d** > **4e** > **4f**; **4g** > **4h** > **4i**. Moreover, di-halogen substituents (**4s** and **4t**) seem to be unfavorable to anti-WT-HIV-1 activities as compared to their monofluorinated analogues.

For compounds **4j-l** bearing a methyl, the position priority is as follows, meta- > ortho- > para-. Among which, meta-methyl derivative **4k** displayed an excellent activity against WT HIV-1 (EC_{50} = 8.8 nM) and a high SI of 3409. The compounds **4m-o** with a methoxyyl seemed to be inferior to the corresponding compounds **4j-l** with a methyl in the same position. Trifluoromethyl, another versatile group in medicinal chemistry, [22, 23] was also introduced to *ortho*- and *meta*-position. However, it was proven to be disadvantageous to activities by **4p** (EC_{50} = 1.7 μM) bearing a *ortho*-CF_3 and **4q** (EC_{50} = 0.61 μM) bearing a *meta*-CF_3. When the cyano group (-CN) was introduced at different positions, only introduction of an *ortho*-CN engenders an activity superior to the unsubstituted phenyl derivative, while *meta*- or *para*-CN both led to a loss of activities. Replacing the phenyl wing in **4x** by a 1-naphtyl neither changes the inhibitory activity nor the cytotoxicity markedly, whereas the 2-naphtyl is approximately 8-fold less active than the phenyl derivative, but has the advantage of being 17 fold less cytotoxic. The wing α of target molecules was also modified with heteroaryls such as pyridinyl and pyrimidinyl. Unexpectedly, the compound **4ab** (EC_{50} = 7.6 nM) bearing a 2-pyridinyl was over 100-fold more potent than **4aa** (EC_{50} = 0.77 μM) with a 3-pyridinyl. As could be expected, the byproduct **4ad**, missing the wing I, was the weakest of all compounds.

To investigate the potency against drug-resistant virus, all compounds were evaluated for their activity against the RT mutant (E138K), the primary mutation in resistance to rilpivirine and double RT mutant (K103N + Y181C) HIV-1 strains which is cross-resistant to most of currently available NNRTIs.[25, 26] As shown in Table 1, four compounds (**4g**, **4r**, **4y**, **4ab**) exhibited moderate activities with EC_{50} values of less than 1 μM against E138K mutant. And nearly all compounds are devoid of activities against double RT mutant (K103N + Y181C) HIV-1 strain.

In this work, all compounds were also evaluated for their activities against HIV-2 (ROD) in MT-4 cells. It is not unexpected that all compounds are lack of activity against HIV-2. As well-known most of previously discovered NNRTIs[9, 27-28] are only active against HIV-1 and lack of anti-HIV-2 activity, though HIV-1 and HIV-2 reverse transcriptases are similar in structure and functionality.[29-31]

2.3 Molecular modeling analysis

To investigate the binding mode of our newly synthesized compounds, molecular modeling was

ACCEPTED MANUSCRIPT

carried out using the software SYBYL Surflex-Dock program and crystal structure of WT HIV-1 RT/TMC125 (PDB code: 3MEC). Compounds **4r** and **4ab** were docked into the HIV-1 RT nonnucleoside binding site (NNBS) (Fig. 2). As illustrated in Fig. 2, compounds **4r** and **4ab** displayed similar binding mode as TMC125 and its analogue in NNBS，adopting the expected "horseshoe" conformation. 1). The left ring of compound **4r** and **4ab** and the aromatic amino acid residues Tyr181, Tyr188 and Trp229 generated π-π stacking interaction. 2) The NH group of compound **4r** and **4ab** formed a key hydrogen bond with the mainchain carbonyl of Lys101 and Leu100. 3) The para-substituted CN of right wing extended to surface of solvent and protein and interacted with amino acid residue Pro236 and Lys103.

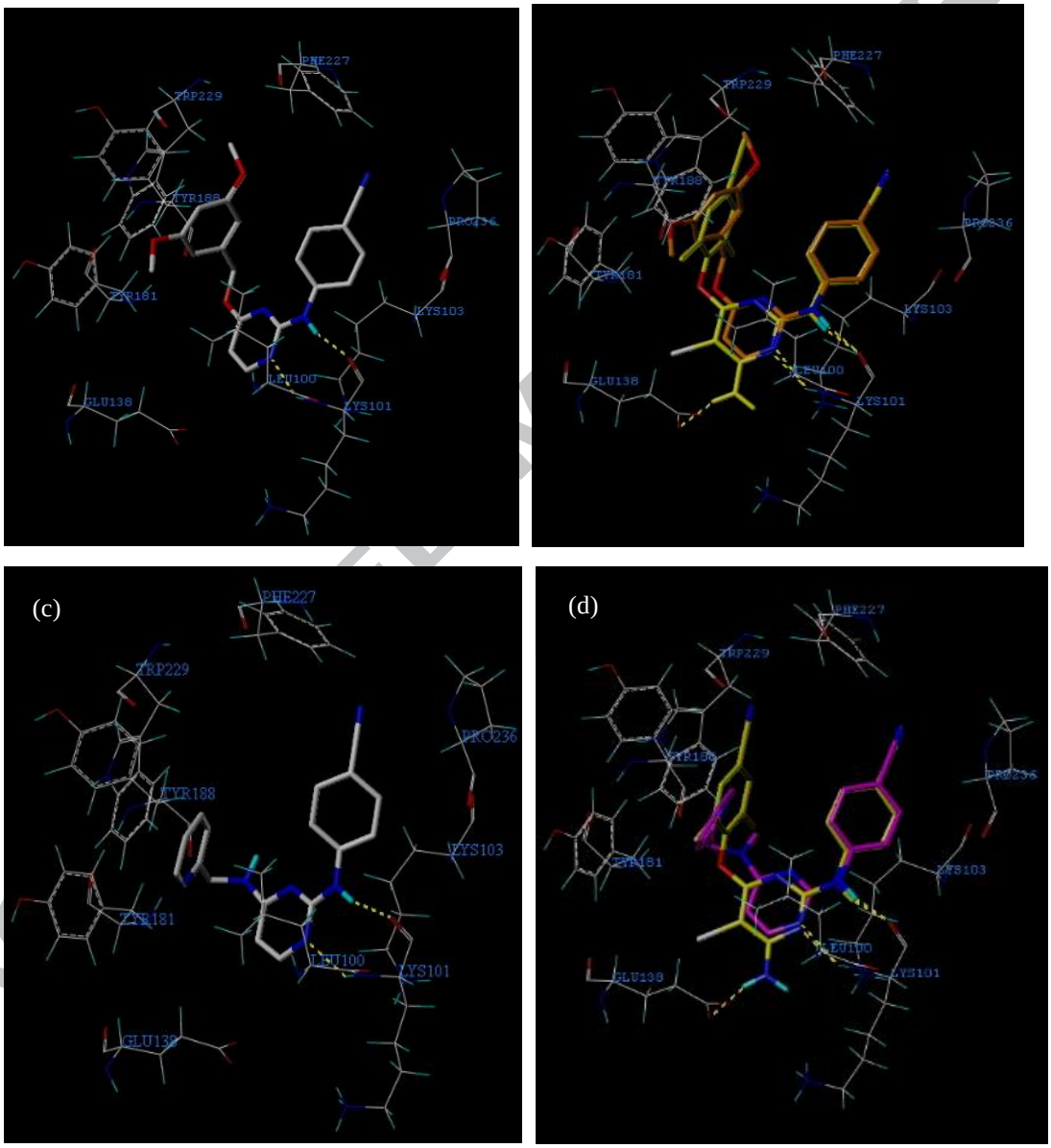

Fig. 2 (a) Docking studies of **4r** into NNBS; (b) Binding mode of **4r** (orange) and overlap with TMC125 (yellow) in NNBS; (c) Docking studies of **4ab** into NNBS; (d) Binding mode of **4ab** (violet) and overlap with TMC125 (yellow) in NNBS. (PDB code: 3MEC)

On the other hand, as illustrated in Fig. 2, the binding mode of **4ab** (with no substitutes at the left wing) is totally different from TMC125. The 2,6-dimethyl-4-cyano fragment of TMC125 could form extensive interactions with surrounding hydrophobic sub-pocket defined by Trp229

ACCEPTED MANUSCRIPT

and Phe227 which may improve the binding affinity and thereby benefit for the anti-HIV-1 activity. Methoxy groups substituted at left wing of **4r** cannot form strong π-π stacking with amino acid residues like 2,6-dimethyl-4-cyano, that might account for that **4ab** and **4r** series showed inferior double mutants activity. It is clear that hydrogen bond formed between TMC125 and Glu138, however, no similar hydrogen bond formed between **4r** (or **4ab**) and Glu138. That might account for why **4r** and **4ab** were not active to double mutant strains.

3. Conclusion

In conclusion, as a continuing effort to find new NNRTIs, a series of structurally diverse analogues of diarylpyrimidines were synthesized. The modifications involved not only the linker but also the wing α of DAPYs. The anti-HIV-1 activities of all target molecules were evaluated, and some of them exhibited excellent anti-HIV-1 (WT) activities and extremely low cytotoxicities. Among which, compound **4g** showed excellent activity against WT HIV-1 with an EC_{50} value of 5.8 nM, HIV-1 mutant (E138K) with an EC_{50} value of 0.30 μM and SI of up to 26108. And compound **4ab** with a novel pyridinyl Wing α displayed activites against WT HIV-1 with an EC_{50} value of 7.6 nM, HIV-1 mutant (E138K) with an EC_{50} value of 0.24 μM, and SI of 1113. The SAR was also summarized, which constitutes a foundation for the further development of new DAPYs as NNRTIs.

4. Experimental

4.1 Chemistry

Melting points were measured on a SGW X-1 microscopic melting-point apparatus. Nuclear magnetic resonance (NMR) spectra on two Varian spectrometers (400M or 600 MHz for ^{1}H NMR; 100 MHz or 150 MHz for ^{13}C NMR; 564MHz for ^{19}F NMR) were recorded in DMSO-d_6. Chemical shifts were reported in δ (ppm) units relative to the internal standard tetramethylsilane. Mass spectra were obtained on a Waters Quattro Micromass instrument using electrospray ionization (ESI) techniques. Elemental analyses were performed on a Carlo Erba 1106 instrument. All chemicals and solvents were of reagent grade and were purified and dried by standard methods before use. All the reactions were monitored by thin layer chromatography (TLC) on pre-coated silica gel G plates at 254 nm under a UV lamp. Column chromatography separations were performed on silica gel (300–400 mesh).

4.1.1 Synthesis of the intermediate 2-(methylthio)pyrimidin-4(1*H*)-one(6)

Methyl iodide (85.16 g, 0.60 mol) was added dropwise to a solution of 2-thiouracil (64.07 g, 0.50 mol), sodium hydroxide (20.8 g, 0.52 mol) in H_2O (400 mL) in 20 min at 10 °C. The mixture was stirred at room temperature for 14 h, then cooled to 5 °C. The precipitates were filtered, washed with water, and dried to obtain 2-(methylthio)pyrimidin-4(1*H*)-one (**6**) as a white solid, 58.72 g, yield 82.6%, mp 200–201 °C (lit. 200–201 °C).

4.1.2 Synthesis of the intermediate 4-((4-oxo-1,4-dihydropyrimidin-2-yl) amino)benzonitrile (7)

The mixture of **6** (45.50 g, 0.32 mol) and 4-cyanoaniline (113.41 g, 0.96 mol) was slowly heated to 180–190 °C and maintained at this temperature for 10 h. After cooling, the hard mixture was crushed by ultrasound treatment in CH_3CN (300 mL). Then the solid was filtered off and washed with CH_3CN until no residual 4-cyanoaniline was detected by TLC to afford 4-((4-oxo-1,4-dihydropyrimidin-2-yl)amino)benzonitrile (**7**) as a light yellow solid (48.96 g, yield 72.1%), which was used directly in next step.

ACCEPTED MANUSCRIPT

4.1.3 Synthesis of the intermediate 4-((4-chloropyrimidin-2-yl) amino)benzonitrile (8)

A mixture of **7** (42.44 g, 0.20 mol) and $POCl_3$ (100 mL) was refluxed for 30 min, then cooled slightly and poured slowly into crushed ice (450 g) under vigorous agitation. The resulting yellow precipitate was filtered. The filter cake was added into chilly water (200 mL), neutralized with sodium hydroxide to pH 7. The mixture was filtered, and the filter cake was dried to get yellow powder, which was added into acetonitrile (90 mL) and stirred for 2 h. The mixture was filtered and dried to give light yellow powder 4-((4-chloropyrimidin-2-yl)amino)benzonitrile (**8**) (32.48 g, 70.4%), which could be used without further purification. Pure **8** as white solid could be afforded by column chromatography using dichloromethane as eluent. Its NMR data can be found in the supplementary data.

4.1.4 Synthesis of target molecules 4a-ac

To a 100 mL two-necked flask was added substituted benzyl alcohol or 4,6-dimethylpyrimidine-2-thiol (2.60 mmol), NaOH (6.40 g, 1.60 mmol) and dimethylsulfoxide (30 mL). The flask was vacuumed and flushed three times with nitrogen. Then the solution of **8** (0.20 g, 0.87 mmol) in dimethylsulfoxide (5～10 mL) was added, and the resulting mixture was heated to 80 ℃ and kept at that temperature for approximately 12 h until the completion of the reaction (monitored by TLC). Subsequently, the mixture was cooled to room temperature and diluted with ethyl acetate (100 mL). The mixture was washed with brine to pH 7, and the organic phase was dried with anhydrous sodium sulfate. The organic phase was concentrated to get crude product, which was purified by column chromatography (ethyl acetate / petroleum ether 1:30 as eluent) to get **4a–ac** in yields of 27.3–75.1%.

4a: white solid, yield 67.1%, mp 207-209 °C; ^{1}H NMR (600 MHz, DMSO-d_6) δ 10.21 (s, 1H, 4-CNArN*H*-), 8.34 (d, 1H, Py*H*), 7.90-7.39 (m, 8H, Ar*H*), 6.52 (d, 1H, Py*H*), 5.52 (s, 2H, -CH_2-); ^{13}C NMR (150 MHz, DMSO-d_6) δ 169.16, 159.40, 159.29, 145.17, 134.18, 133.35, 132.90, 130.40, 130.30, 129.84, 127.86, 119.95, 118.86, 102.93, 100.58, 65.30. MS(ESI) 337.1 $(M+1)^+$.

4b: white solid, yield 40.1%, mp 203-205 °C; ^{1}H NMR (600 MHz, DMSO-d_6) δ 10.16 (s, 1H, 4-CNArN*H*-), 8.33 (d, 1H, Py*H*), 7.90-7.39 (m, 8H, Ar*H*) , 6.50 (d, 1H, Py*H*), 5.44 (s, 2H, -CH_2-); ^{13}C NMR (150 MHz, DMSO-d_6) δ 169.23, 159.28, 159.00, 145.05, 139.32, 133.53, 133.40, 130.84, 128.39, 128.04, 126.87, 119.95, 119.01, 103.01, 100.63, 67.03. MS(ESI) 337.1 $(M+1)^+$.

4c: white solid, yield 66.7%, mp 209-211 °C; ^{1}H NMR (600 MHz, DMSO-d_6) δ 10.12 (s, 1H, 4-CNArN*H*-), 8.32 (d, 1H, Py*H*), 7.93-7.45 (m, 8H, Ar*H*), 6.48 (d, 1H, Py*H*), 5.43 (s, 2H, -CH_2-).; ^{13}C NMR (150 MHz, DMSO-d_6) δ 169.21, 159.43, 159.19, 145.16, 135.83, 133.40, 133.09, 130.22, 128.91, 119.98, 118.88, 102.90, 100.60, 67.02. MS(ESI) 337.1 $(M+1)^+$.

4d: white solid, yield 66.1%, mp 199-201 °C; ^{1}H NMR (600 MHz, DMSO-d_6) δ 10.16 (s, 1H, 4-CNArN*H*-), 8.35 (d, 1H, Py*H*), 7.91-7.30 (m, 8H, Ar*H*), 6.53 (d, 1H, Py*H*), 5.49 (s, 2H, -CH_2-); ^{13}C NMR (150 MHz, DMSO-d_6) δ 169.13, 159.41, 159.31, 145.16, 135.77, 133.37, 133.05, 130.57, 130.22, 128.38, 122.99, 119.96, 118.84, 102.92, 100.57, 67.48. MS(ESI) 383.0 $(M+2)^+$.

4e: white solid, yield 65.7%, mp 190-192 °C; ^{1}H NMR (600 MHz, DMSO-d_6) δ 10.13 (s, 1H, 4-CNArN*H*-),8.32 (d, 1H, Py*H*), 7.92-7.35 (m, 8H, Ar*H*), 6.50 (d, 1H, Py*H*), 5.44 (s, 2H, -CH_2-); ^{13}C NMR (150 MHz, DMSO-d_6) δ 169.16, 159.42, 159.24, 145.13, 139.61, 133.39, 131.28, 131.12, 130.92, 127.24, 122.11, 119.97, 118.93, 102.91, 100.60, 66.93.MS(ESI) 383.0 $(M+2)^+$.

4f: white solid, yield 57%, mp 179-181 °C; ^{1}H NMR (600 MHz, DMSO-d_6) δ 10.12 (s, 1H, 4-CNArN*H*-), 8.32 (d, 1H, Py*H*), 8.31-7.43 (m, 8H, Ar*H*), 6.48 (d, 1H, Py*H*), 5.42 (s, 1*H*, -CH_2-); ^{13}C NMR (150 MHz, DMSO-d_6) δ 169.98, 169.20, 159.56, 159.42, 159.20, 158.79, 145.16, 136.26, 133.40, 131.83, 130.48, 121.62, 119.97, 118.87, 102.90, 100.59, 67.05, 54.09. MS(ESI) 383.0 $(M+2)^+$.

4g: white solid, yield 53.9%, mp 185-187 °C; ^{1}H NMR (600 MHz, DMSO-d_6) δ 10.14 (s, 1H,

ACCEPTED MANUSCRIPT

4-CNArN*H*-), 8.32 (d, 1H, Py*H*), 7.95-7.22 (m, 8H, Ar*H*), 6.47 (d, 1H, Py*H*), 5.49 (s, 2*H*, -CH_2-); ^{13}C NMR (150 MHz, DMSO-d_6) δ 169.17, 161.70 (d, J =243.45 Hz), 159.43, 158.48, 145.24 (d, J =17.25 Hz), 132.88, 131.59 (d, J =8.85 Hz), 131.53, 130.60 (d, J =19.35 Hz), 124.47 (d, J =8.55 Hz), 123.58, 119.97, 119.20, 118.30, 102.98, 101.08, 100.06, 62.08. ^{19}F NMR(564 MHz, DMSO-d_6) δ -118.32. MS(ESI) 321.1 $(M+1)^+$.

4h: white solid, yield 69.5%, mp 224-226 °C; ^{1}H NMR (600 MHz, DMSO-d_6) δ 10.13(s, 1H, 4-CNArN*H*-), 8.33（d, 1H, J = 5.4 Hz）, 7.93-7.19 (m, 8H, Ar*H*), 6.50 (d, 1H, J = 5.4 Hz), 5.45 (s, 2H, -CH_2-); ^{13}C NMR (150 MHz, DMSO-d_6) δ 169.20, 163.38 (d, J =241.65Hz), 159.42, 159.22, 145.16, 139.69 (d, J =7.8 Hz), 133.39, 130.99 (d, J =8.4 Hz), 124.25 (d, J =2.4 Hz), 119.97, 118.90, 115.30 (d, J =20.7 Hz), 115.05(d, J = 21.75 Hz), 102.89, 100.62, 67.02. ^{19}F NMR(564 MHz, DMSO-d_6) δ -113.13. MS(ESI) 321.1 $(M+1)^+$.

4i: white solid, yield 57.1%, mp 179-180 °C; ^{1}H NMR (600 MHz, DMSO-d_6) δ 10.12 (s, 1H, 4-CNArN*H*-), 8.31（d, 1H, J = 5.4 Hz）, 7.92-7.19 (m, 8H, Ar*H*), 6.47 (d, 1H, J = 5.4 Hz), 5.42 (s, 2H, -CH_2-); ^{13}C NMR (150 MHz, DMSO-d_6) δ 169.27, 163.14 (d, J =242.7 Hz), 159.43,159.13, 145.20, 133.41,132.99 (d, J =2.85 Hz), 130.85 (d, J =8.4 Hz), 119.98, 118.88, 115.81 (d, J =21.0 Hz), 102.88, 100.62, 67.19. ^{19}F NMR(564 MHz, DMSO-d_6) δ -114.05. MS(ESI) 321.1 $(M+1)^+$.

4j: white solid, yield 65.3%, mp 185-187 °C; ^{1}H NMR (600 MHz, DMSO-d_6) δ 10.12 (s, 1H, 4-CNArN*H*-), 8.32 (d, 1H, Py*H*), 7.94-7.20 (m, 8H, Ar*H*), 6.48(d, 1H, Py*H*), 5.43 (s, 2H, -CH_2-), 2.33(s, 3H, -CH_3); ^{13}C NMR (150 MHz, DMSO-d_6) δ 169.43, 159.46, 159.10, 145.24, 136.95, 134.66, 133.35, 130.58, 129.02, 128.68, 126.31, 119.98, 118.88, 102.87, 100.56, 66.45, 18.91. MS(ESI) 317.1 $(M+1)^+$.

4k: white solid, yield 64.2%, mp 168-170 °C; ^{1}H NMR (600 MHz, DMSO-d_6) δ 10.11 (s, 1H, 4-CNArN*H*-), 8.30 (d, 1H, Py*H*), 7.95-7.14 (m, 8H, Ar*H*), 6.46 (d, 1H, Py*H*), 5.39 (s, 2H, -CH_2-), 2.30 (s, 3H, -CH_3); ^{13}C NMR (150 MHz, DMSO-d_6) δ 169.37, 159.46, 159.07, 145.22, 138.06, 136.62, 133.37, 129.10, 128.99, 128.80, 125.51, 119.99, 118.91, 102.85, 100.62, 67.93, 21.37. MS(ESI) 317.1 $(M+1)^+$.

4l: white solid, yield 75.1%, mp 170-172 °C; ^{1}H NMR (600 MHz, DMSO-d_6) δ 10.10 (s, 1H, 4-CNArN*H*-), 8.30 (d, 1H, Py*H*), 7.95- 7.19 (m, 8H, Ar*H*), 6.45 (d, 1H, Py*H*), 5.39 (s, 2H, -CH_2-), 2.29 (s, 3H, -CH_3); ^{13}C NMR (150 MHz, DMSO-d_6) δ 169.38, 159.45, 159.05, 145.23, 137.81, 133.68, 133.39, 129.43, 128.55, 119.99, 118.88, 102.85, 100.64, 67.81, 21.20. MS(ESI) 317.1 $(M+1)^+$.

4m: white solid, yield 69.2%, mp 175-177 °C; ^{1}H NMR (600 MHz, DMSO-d_6) δ 10.10 (s, 1H, 4-CNArN*H*-), 8.31 (d, 1H, Py*H*), 7.95-6.96 (m, 8H, Ar*H*), 6.47 (d, 1H, Py*H*), 5.42 (s, 2H, -CH_2-), 3.82 (s, 3H, -OCH_3); ^{13}C NMR (150 MHz, DMSO-d_6) δ 169.50, 159.46, 158.96, 157.53, 145.29, 133.34, 130.07, 129.67, 124.33, 120.70, 119.98, 118.85, 111.28, 102.84, 100.68, 63.53, 55.88. MS(ESI) 333.2 $(M+1)^+$.

4n: white solid, yield 61.8%, mp 154-155 °C; ^{1}H NMR (600 MHz, DMSO-d_6) δ 10.11 (s, 1H, 4-CNArN*H*-), 8.31 (d, 1H, Py*H*), 7.94-6.90 (m, 8H, Ar*H*), 6.48 (d, 1H, Py*H*), 5.41 (s, 2H, -CH_2-), 3.74 (s, 3H, -OCH_3); ^{13}C NMR (150 MHz, DMSO-d_6) δ 169.33, 159.75, 159.44, 159.13, 145.20, 138.29, 133.38, 130.04, 120.47, 119.97, 118.89, 113.94, 113.89, 102.86, 100.63, 67.75, 55.48. MS(ESI) 333.2 $(M+1)^+$.

4o: white solid, yield 70.1%, mp189-191 °C; ^{1}H NMR (600 MHz, DMSO-d_6) δ 10.07 (s, 1H, 4-CNArN*H*-), 8.30 (d,1H, Py*H*), 7.97-6.94 (m, 8H, Ar*H*), 6.40 (d, 1H, Py*H*), 5.36 (s, 2H, -CH_2-), 3.75 (s, 3H, -OCH_3); ^{13}C NMR (150 MHz, DMSO-d_6) δ 169.40, 159.64, 159.45, 159.00, 145.26, 133.41, 130.43, 128.55, 120.00, 118.88, 114.28, 102.84, 100.66, 67.75, 55.54. MS(ESI) 333.2 $(M+1)^+$.

ACCEPTED MANUSCRIPT

4p: white solid, yield 46.4%, mp168-170 °C; ^{1}H NMR (600 MHz, DMSO-d_6) δ 10.13 (s, 1H,4-CNArN*H*-), 8.34 (d, 1*H*), 7.92-7.57 (m, 8H, Ar*H*), 6.48 (d, 1H, Py*H*), 5.59 (s, 2H, -CH_2-); ^{13}C NMR (150 MHz, DMSO-d_6) δ 169.03, 159.42, 159.27, 145.13, 134.58, 133.25, 130.75, 129.23, 127.34 (d, *J* =30.6 Hz), 126.59 (d, *J* =5.25 Hz), 126.55 (d, *J* =5.70 Hz), 125.62 (d, *J* =272.55 Hz), 119.91, 118.89, 102.98, 100.53, 64.44. ^{19}F NMR(564 MHz, DMSO-d_6) δ -58.75. MS(ESI) 371.2 $(M+1)^+$.

4q: white solid, yield48.1%, mp 168-170 °C; ^{1}H NMR (600 MHz, DMSO-d_6) δ 10.13 (s, 1H, 4-CNArN*H*-), 8.33 (d,1*H*), 7.93-7.63 (m, 8H, Ar*H*), 6.51 (d, 1*H*), 5.54 (s, 2H, -CH_2-); ^{13}C NMR (150 MHz, DMSO-d_6) δ 169.17, 159.43, 159.26, 145.13, 138.30, 133.36, 132.38, 130.03, 129.75 (d, *J* =30.5 Hz), 125.45 (d, *J* =270.9 Hz), 125.17 (d, *J* =4.05 Hz), 124.86 (d, *J* =3.6 Hz),119.94, 118.94, 102.93, 100.56, 67.05. ^{19}F NMR(564 MHz, DMSO-d_6) δ -61.15. MS(ESI) 371.1 $(M+1)^+$.

4r: white solid, yield 71.6%, mp 155-157 °C; ^{1}H NMR (600 MHz, DMSO-d_6) δ 10.11 (s, 1H, 4-CNArN*H*-), 8.31-6.62 (m, 10H, Ar*H*+Py*H*), 5.36 (s, 2H, -CH_2-), 3.73 (s, 6H, -OCH_3);^{13}C NMR (150 MHz, DMSO-d_6) δ 169.31, 160.96, 159.43, 159.14, 145.20, 139.03, 133.37, 119.97, 118.91, 106.25, 102.86, 100.62, 100.06, 67.78, 55.62. MS(ESI) 363.3 $(M+1)^+$.

4s: white solid, yield 45.7%, mp 213-215 °C; ^{1}H NMR (600 MHz, DMSO-d_6) δ 10.16 (s, 1H, 4-CNArN*H*-), 8.35-6.56 (m, 9H, Ar*H*+Py*H*), 5.45 (s, 2H, -CH_2-). ^{13}C NMR (150 MHz, DMSO-d_6) δ 168.93, 162.71 (d, *J* =243.75 Hz), 159.37, 145.13, 138.36 (d, *J* =7.95 Hz), 134.76 (d, *J* =7.95 Hz), 133.34, 119.93, 118.85, 117.46 (d, *J* =22.05 Hz), 117.08 (d, *J* =2.55 Hz), 116.91 (d, *J* =23.85 Hz), 102.98, 100.59, 66.94. ^{19}F NMR(564 MHz, DMSO-d_6) δ -114.12. MS(ESI) 401.0 $(M+2)^+$

4t: white solid, yield 45.0%, mp 211-214 °C; ^{1}H NMR (600 MHz, DMSO-d_6) δ 10.13 (s, 1H, 4-CNArN*H*-), 8.33 (d, 1H, Py*H*), 7.94-7.45 (m, 7H, Ar*H*), 6.47 (d, 1H, Py*H*), 5.46 (s, 2H, -CH_2-); ^{13}C NMR (150 MHz, DMSO-d_6) δ 169.02, 161.53(d, *J* =250.35 Hz), 159.37, 159.26, 145.14, 133.37, 132.57 (d, *J* =4.50 Hz), 128.21 (d, *J* =3.45 Hz), 123.41 (d, *J* =14.85 Hz), 122.40 (d, *J* =9.3 Hz), 119.94, 119.41 (d, *J* =24.15 Hz), 118.91, 102.98, 100.56, 61.59. ^{19}F NMR(564 MHz, DMSO-d_6) δ -115.03. MS(ESI) 401.0 $(M+2)^+$.

4u: white solid, yield 27.3%, mp 252-254 °C; ^{1}H NMR (600 MHz, DMSO-d_6) δ 10.15 (s, 1H, 4-CNArN*H*-), 8.33 (d, 1H, Py*H*), 8.08-7.49 (m, 8H, Ar*H*), 6.49 (d, 1H, Py*H*), 5.91 (s, 2H, -CH_2-); ^{13}C NMR (150 MHz, DMSO-d_6) δ 169.39, 159.48, 159.20, 145.19, 133.69, 133.30, 132.24, 129.27, 129.02, 127.08, 126.48, 125.85, 124.04, 118.88, 102.83, 100.64, 66.24. MS(ESI) 328.1 $(M+1)^+$.

4v: white solid, yield 34.5%, mp 220-222 °C; ^{1}H NMR (600 MHz, DMSO-d_6) δ 10.13 (s, 1H, 4-CNArN*H*-), 8.33 (d, 1H, Py*H*), 8.00-7.51 (m, 8H, Ar*H*), 6.51 (d, 1H, Py*H*), 5.61 (s, 2H, -CH_2-); ^{13}C NMR (150 MHz, DMSO-d_6) δ 168.98, 159.07, 158.77, 144.79, 133.97, 132.99, 132.75, 132.60, 128.14, 127.79, 126.65, 126.42, 125.84, 119.58, 118.51, 102.47, 100.26, 67.60.

4w: white solid, yield31.2%, mp 225-228 °C; ^{1}H NMR (600 MHz, DMSO-d_6) δ 10.18 (s, 1H, 4-CNArN*H*-), 8.36 (d, 1H, Py*H*), 7.96-7.57 (m, 8H, Ar*H*), 6.54 (d, 1H, Py*H*), 5.62 (s, 2H, -CH_2-); ^{13}C NMR (150 MHz, DMSO-d_6) δ 168.59, 158.99, 144.70, 139.56, 133.56, 133.25, 132.97, 129.25, 119.52, 118.49, 117.13, 110.94, 102.55, 100.11, 65.38.

4x: white solid, yield 70.4%, mp 178-180 °C; ^{1}H NMR (400 MHz, DMSO-d_6) δ 10.12 (s, 1H, 4-CNArN*H*-), 8.32 (d, 1H, Py*H*), 7.94-7.35 (m, 9H, Ar*H*), 6.49 (d, 1H, Py*H*), 5.44 (s, 2H, -CH_2-); ^{13}C NMR (150 MHz, DMSO-d_6) δ 169.28, 159.44, 159.20, 145.16, 136.99, 134.91, 133.41, 131.02, 128.88, 119.98, 118.87, 102.88, 100.64, 67.58. MS(ESI) 303.64 $(M+1)^+$.

4y: white solid, yield 37.7%, mp 168-170 °C; ^{1}H NMR (400 MHz, DMSO-d_6) δ 10.13 (s, 1H, 4-CNArN*H*-), 8.33 (d, 1H, Py*H*), 8.09-7.49 (m, 11H, Ar*H*), 6.50 (d, 1H, Py*H*), 5.92 (s, 2H, -CH_2-). MS(ESI) 353.2 $(M+1)^+$.

ACCEPTED MANUSCRIPT

4z: white solid, yield 31.9%, mp 196-197 °C; ^{1}H NMR (400 MHz, DMSO-d_6) δ 10.11 (s, 1H, 4-CNArN*H*-), 8.33 (d, 1H, Py*H*), 8.00-7.51 (m, 11H, Ar*H*), 6.51 (d, 1H, Py*H*), 5.61 (s, 2H, -CH_2-). MS(ESI) 353.1(M+1)$^+$.

4aa: white solid, yield 50.8%, mp 207-209 °C; ^{1}H NMR (400 MHz, DMSO-d_6) δ 10.15 (s, 1H, 4-CNArN*H*-), 8.72-7.42 (m, 9H, Ar*H*+Py*H*), 6.48 (d, 1H, Py*H*), 5.48 (s, 2H, -CH_2-). MS(ESI) 304.2(M+1)$^+$.

4ab: white solid, yield 43.2%, mp 193-195 °C; ^{1}H NMR (400 MHz, DMSO-d_6) δ 9.58 (s, 1H, 4-CNArN*H*-), 8.57-7.24 (m, 10H, Ar*H*+Py*H*), 6.19 (s, 1H, -CH$_2$N*H*-), 4.65 (s, 2H, -CH_2-). MS(ESI) 303.1 (M+1)$^+$.

4ac: white solid, yield 53.6%, mp 237-239 °C; ^{1}H NMR (400 MHz, DMSO-d_6) δ 10.36 (s, 1H, 4-CNArN*H*-), 8.49 (d, 1H, Py*H*), 7.86-7.67 (d, 4H, Ar*H*), 7.58 (d, 1H, Py*H*), 7.24 (s, 1H, Py*H*), 2.42 (s, 6H, -CH_3). MS(ESI) 334.36 (M+1)$^+$.

4.1.5 Synthesis of byproduct 4ad

To a 50 mL necked flask was added ammonium hydroxide (6.5 mL), compound **8** (0.434mmol) and dimethylformamide (8 mL). The mixture was heated 140 °C for approximate 6.5 h until the completion of the reaction (monitored by TLC). Subsequently, the mixture was cooled to room temperature and poured into water (100 mL), extracted with ethyl acetate. The organic phase was dried with anhydrous sodium sulfate, and concentrated to get crude product, which was purified by column chromatography (ethyl acetate / petroleum ether 1:30 as eluent) to get **4ad**. White solid, yield 92.3%, mp 200-203 °C; ^{1}H NMR (400 MHz, CDCl$_3$) δ 7.99 (d, 1H, Py*H*), 7.76 (d, 2H, Ar*H*), 7.65 (s, 1H, 4-CNArN*H*-), 7.56 (d, 2H, Ar*H*), 6.05 (d, 1H, Py*H*), 3.12 (s, 6H, -NCH_3). MS(ESI) 240.1 (M+1)$^+$.

4.2 Anti-HIV activity assay

4.2.1 Anti-HIV activity assay in MT-4 cells

The anti-HIV activity and cytotoxicity of the target molecules were evaluated against wild-type (WT) HIV-1 strain III$_B$, RT mutant (E138K), double RT mutant (K103N + Y181C) HIV-1 (RES056) and HIV-2 strain ROD in MT-4 cell cultures using the 3-(4,5-dimethylthiazol-2-yl)-2,5-diphenyltetrazolium bromide (MTT) method.[21, 22] Briefly, stock solutions (10 x final concentration) of test compounds were added in 25 µL volumes to two series of triplicate wells so as to allow simultaneous evaluation of their effects on mock-and HIV-infected cells at the beginning of each experiment. Serial 5-fold dilutions of test compounds were made directly in flat-bottomed 96-well microtiter trays using a Biomek 3000 robot (Beckman instruments, Fullerton, CA). Untreated control HIV-and mock-infected cell samples were included for each sample. Virus stock (50 µL) at 100-300 CCID$_{50}$ (50% cell culture infectious dose) or culture medium was added to either the virus-infected or mock-infected wells of the microtiter tray. Mock-infected cells were used to evaluate the effect of test compounds on uninfected cells in order to assess the cytotoxicity of the test compounds. Exponentially growing MT-4 cells were centrifuged for 5 min at 1,000 rpm (220 g) and the supernatant was discarded. The MT-4 cells were resuspended at 6 x 10^5 cells/mL and 50-µL volumes were transferred to the microtiter tray wells. Five days after infection, the viability of mock-and HIV-infected cells was examined spectrophotometrically by the MTT assay.

The MTT assay is based on the reduction of yellow colored 3-(4,5-dimethylthiazol-2-yl)-2,5-diphenyltetrazolium bromide (MTT) (Acros Organics) by mitochondrial dehydrogenase activity in metabolically active cells to a blue-purple formazan that can be measured spectrophotometrically. The absorbances were read in an eight-channel computer-controlled photometer (Infinite M1000, Tecan), at

ACCEPTED MANUSCRIPT

two wavelengths (540 and 690 nm). All data were calculated using the median absorbance value of three wells. The 50% cytotoxic concentration (CC_{50}) was defined as the concentration of the test compound that reduced the absorbance (OD_{540}) of the mock-infected control sample by 50%. The concentration achieving 50% protection against the cytopathic effect of the virus in infected cells was defined as the 50% effective concentration (EC_{50}).

4.2.2 Molecular docking

Molecular modeling was performed with the Tripos molecular modeling packages Sybyl-X 1.2. All the molecules for docking were built using standard bond lengths and angles from Sybyl-X 1.2/base Builder and were then optimized using the Tripos force field for 2,000 generations two times or more, until the minimized conformers of the ligand were the same. The flexible docking method, called Surflex-Dock, docks the ligand automatically into the ligand binding site of the receptor by using a protocol-based approach and an empirically-derived scoring function.[32-34] The protocol is a computational representation of a putative ligand that binds to the intended binding site and is a unique and essential element of the docking algorithm. The scoring function in Surflex-Dock, which contains hydrophobic, polar, repulsive, entropic, and solvation terms, was trained to estimate the dissociation constant (K_d) expressed in -log $(K_d)^2$. Prior to docking, the protein was prepared by removing water molecules, the ligand (TMC120), and other unnecessary small molecules from the crystal structure of the TMC125-HIV-1 RT complex (PDB code: 3MEC)[35]; simultaneously, polar hydrogen atoms were added to the protein. Surflex-Dock default settings were used for other parameters, such as the number of starting conformations per molecule (set to 0), the size to expand search grid (set to 8Å), the maximum number of rotatable bonds per molecule (set to 100), and the maximum number of poses per ligand (set to 20). During the docking procedure, all of the single bonds in residue side-chains inside the defined RT binding pocket were regarded as rotatable or flexible, and the ligand was allowed to rotate at all single bonds and move flexibly within the tentative binding pocket. The atomic charges were recalculated using the Kollman all-atom approach for the protein and the Gasteiger–Hückel approach for the ligand. The binding interaction energy was calculated to include van der Waals, electrostatic, and torsional energy terms defined in the Tripos force field. The structure optimization was performed for 20,000 generations using a genetic algorithm, and the 20-best-scoring ligand–protein complexes were kept for further analyses. The $-\log (K_d)^2$ values of the 20-best-scoring complexes, which represented the binding affinities of ligand with RT, encompassed a wide scope of functional classes (10^{-2}-10^{-9}). Therefore, only the highest-scoring 3D structural model of the ligand-bound RT was chosen to define the binding interaction[36-39].

Acknowledgements

The financial support from the National Natural Science Foundation of China (No. 21402148, No. 21602164), the Hubei Provincial Department of Education of China (No. XD2014154), Wuhan Institute of Technology Scientific Research Fund (No. K201441, No. K201304), Wuhan Institute of Technology Teaching Research Project (No. X2015014), and Wuhan Institute of Technology President Fund (No. 2016079), is gratefully acknowledged. The authors wish to thank Kristien Erven, and Kris Uyttersprot (Rega) for dedicated technical assistance.

Supplementary data

Supplementary data (^{1}H NMR, ^{13}C NMR, ^{19}F NMR) associated with this article can be found in the

ACCEPTED MANUSCRIPT

online version.

References and notes

1. UNAIDS AIDS by the numbers. http://www.unaids.org/sites/default/files/media_asset/AIDS-by-the-numbers-2016_en.pdf.
2. Palella, F. J.; Delaney, K. M.; Moorman, A. C.; Loveless, M. O.; Fuhrer, J.; Satten, G. A.; Aschman, D. J.; Holmberg, S. D. *N. Engl. J. Med.* **1998**, *338*, 853.
3. Palella, F. J.; Baker, R. K.; Moorman, A. C.; Chmiel, J. S.; Wood, K. C.; Brooks, J. T.; Holmberg, S. D. *J. Acquir. Immune Defic. Syndr.* **2006**, *43*, 27.
4. Chesney, M. *AIDS Patient Care St* **2003**, *17*, 169.
5. De Clercq, E. *Curr. Med. Chem.* **2001**, *8*, 1543.
6. Gu, S.-X.; Xue, P.; Ju, X.-L.; Zhu, Y.-Y. *Bioorg. Med. Chem.* **2016**. *24*, 5007.
7. Mehellou, Y.; De Clercq, E. *J. Med. Chem.* **2010**, *53*, 521.
8. Zhan, P.; Liu, X.; Li, Z.; Pannecouque, C.; De Clercq, E. *Curr. Med. Chem.* **2009**, *16*, 3903.
9. Chen, X.; Zhan, P.; Li, D.; De Clercq, E.; Liu, X. *Curr. Med. Chem.* **2011**, *18*, 359.
10. Udier-Blagovic, M.; Tirado-Rives, J.; Jorgensen, W. L. *J. Am. Chem. Soc.* **2003**, *125*, 6016.
11. Janssen, P. A. J.; Lewi, P. J.; Arnold, E.; Daeyaert, F.; de Jonge, M.; Heeres, J.; Koymans, L.; Vinkers, M.; Guillemont, J.; Pasquier, E.; Kukla, M.; Ludovici, D.; Andries, K.; de Béthune, M. P.; Pauwels, R. D., K.; Clark Jr., A. D.; Frenkel, Y. V.; Hughes, S. H.; Medaer, B.; De Knaep, F.; Bohets, H.; De Clerck, F.; Lampo, A.; Williams, P.; Stoffels, P. *J. Med. Chem.* **2005**, *48*, 1901.
12. Ludovici, D. W.; De Corte, B. L.; Kukla, M. J.; Ye, H.; Ho, C. Y.; Lichtenstein, M. A.; Kavash, R. W.; Andries, K.; de Béthune, M.-P.; Azijn, H.; Pauwels, R.; Lewi, P.; Heeres, J.; Koymans, L. M. H.; de Jonge, M. R.; Van Aken, K. J. A.; Daeyaert, F. F. D.; Das, K.; Arnold, E.; Janssen, P. A. J. *Bioorg. Med. Chem. Lett.* **2001**, *11*, 2235.
13. Rotili, D.; Tarantino, D.; Artico, M.; Nawrozkij, M. B.; Gonzalez-Ortega, E.; Clotet, B.; Samuele, A.; Esté, J. A.; Maga, G.; Mai, A. *J. Med. Chem.* **2011**, *54*, 3091.
14. Gu, S.-X.; He, Q.-Q.; Yang, S.-Q.; Ma, X.-D.; Chen, F.-E.; De Clercq, E.; Balzarini, J.; Pannecouque, C. *Bioorg. Med. Chem.* **2011**, *19*, 5117.
15. Gu, S.-X.; Li, Z.-M.; Ma, X.-D.; Yang, S.-Q.; He, Q.-Q.; Chen, F.-E.; De Clercq, E.; Balzarini, J.; Pannecouque, C. *Eur. J. Med. Chem.* **2012**, *53*, 229.
16. Zeng, Z.-S.; Liang, Y.-H.; Feng, X.-Q.; Chen, F.-E.; Pannecouque, C.; Balzarini, J.; De Clercq, E. *ChemMedChem* **2010**, *5*, 837.
17. Gu, S.-X.; Qiao, H.; Zhu, Y.-Y.; Shu, Q.-C.; Liu, H.; Ju, X.-L.; De Clercq, E.; Balzarini, J.; Pannecouque, C. *Bioorg. Med. Chem.* **2015**, *23*, 6587.
18. Gu, S.-X.; Zhu, Y.-Y.; Chen, F.-E.; De Clercq, E.; Balzarini, J.; Pannecouque, C. *Med. Chem. Res.* **2015**, *24*, 220.
19. Gu, S.-X.; Yang, S.-Q.; He, Q.-Q.; Ma, X.-D.; Chen, F.-E.; Dai, H.-F.; De Clercq, E.; Balzarini, J.; Pannecouque, C. *Bioorg. Med. Chem.* **2011**, *19*, 7093.
20. Ding, S.; Jiao, N. *Angew. Chem.* **2012**, *51*, 9226.
21. Pauwels, R.; Balzarini, J.; Baba, M.; Snoeck, R.; Schols, D.; Herdewijn, P.; Desmyter, J.; De Clercq, E. *J. Virol. Methods* **1988**, *20*, 309.
22. Pannecouque, C.; Daelemans, D.; De Clercq, E. *Nat. Protocols* **2008**, *3*, 427.
23. Purser, S.; Moore, P. R.; Swallow, S.; Gouverneur, V. *Chem. Soc. Rev.* **2008**, *37*, 320.
24. Hagmann, W. K. *J. Med. Chem.* **2008**, *51*, 4359.
25. Chan, J. H.; Freeman, G. A.; Tidwell, J. H.; Romines, K. R.; Schaller, L. T.; Cowan, J. R.;

ACCEPTED MANUSCRIPT

Gonzales, S. S.; Lowell, C. W.; Andrews III, C.; Reynolds, D. J.; St. Clair, M.; Hazen, R. J.; Ferris, R. G.; Creech, K. L.; Roberts, G. B.; Short, S. A.; Weaver, K.; Koszalka, G. W.; Boone., L. R. *J. Med. Chem.* **2004**, *47*, 1175.

26. Miller, V.; De Béthune, M. P.; Kober, A.; Sturmer, M.; Hertogs, K.; Pauwels, R.; Stoffels, P.; Staszewski, S. *Antimicrob. Agents Chemother.* **1998**, *42*, 3123.
27. Zhan, P.; Liu, X. *Expert Opin. Ther. Patents* **2011**, *21*, 717.
28. Gu, S.-X.; Zhang, X.; He, Q.-Q.; Yang, L.-M.; Ma, X.-D.; Zheng, Y.-T.; Yang, S.-Q.; Chen, F.-E. *Bioorg. Med. Chem.* **2011**, *19*, 4220.
29. Witvrouw, M.; Pannecouque, C.; Van Laethem, K.; Desmyter, J.; De Clercq, E.; Vandamme, A. M. *AIDS* **1999**, *13*, 1477.
30. Witvrouw, M.; Pannecouque, C.; Switzer, W. M.; Folks, T. M.; De Clercq, E.; Heneine, W. *Antiv. Ther.* **2004**, *9*, 57.
31. Dang, Z.; Lai, W.; Qian, K.; Ho, P.; Lee, K.-H.; Chen, C.-H.; Huang, L. *J. Med. Chem.* **2009**, *52*, 7887.
32. Jain, A. N., Scoring noncovalent protein-ligand interactions: a continuous differentiable function tuned to compute binding affinities. *J. Comput. Aided Mol. Des.* **1996**, *10* (5), 427-440.
33. Jain, A. N., Surflex: fully automatic flexible molecular docking using a molecular similarity-based search engine. *J. Med. Chem.* **2003**, *46* (4), 499-511.
34. Liu, Q.; Masek, B.; Smith, K.; Smith, J., Tagged fragment method for evolutionary structure-based de novo lead generation and optimization. *J. Med. Chem.* **2007**, *50* (22), 5392-5402.
35. Lansdon, E. B.; Brendza, K. M.; Hung, M.; Wang, R.; Mukund, S.; Jin, D.; Birkus, G.; Kutty, N.; Liu, X., Crystal Structures of HIV-1 Reverse Transcriptase with Etravirine (TMC125) and Rilpivirine (TMC278): Implications for Drug Design. *J. Med. Chem.* **2010,** *53*(10), 4295-4299.
36. Chen, J. Z.; Wang, J.; Xie, X. Q., GPCR structure-based virtual screening approach for CB2 antagonist search. *J. Chem Inf. Model.* **2007**, *47* (4), 1626-1637.
37. Raduner, S.; Majewska, A.; Chen, J. Z.; Xie, X. Q.; Hamon, J.; Faller, B.; Altmann, K. H.; Gertsch, J., Alkylamides from Echinacea are a new class of cannabinomimetics. *J. Biol. Chem.* **2006**, *281* (20), 14192-14206.
38. Ruppert, J.; Welch, W.; Jain, A. N., Automatic identification and representation of protein binding sites for molecular docking. *Protein Sci.* **1997**, *6* (3), 524-533.
39. Welch, W.; Ruppert, J.; Jain, A. N., Hammerhead: fast, fully automated docking of flexible ligands to protein binding sites. *Chem. Biol.* **1996**, *3* (6), 449-462.

ACCEPTED MANUSCRIPT

Graphical abstract

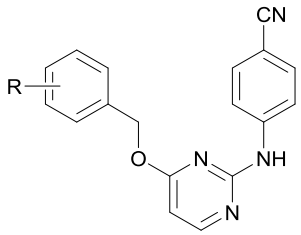

4a-x

4g, R=2-F, $EC_{50}(III_B)$=5.8nM

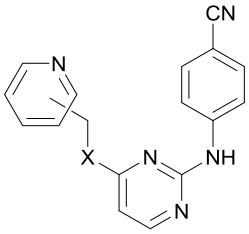

4aa, 3-pyridinyl, X=O;

4ab, 2-pyridinyl, X=N, $EC_{50}(III_B)$=7.6nM

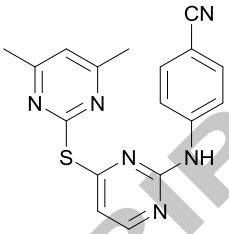

4ac

ACCEPTED MANUSCRIPT